

RADIO OBSERVATIONS OF WEAK ENERGY RELEASES IN THE SOLAR CORONA

R. RAMESH¹, C. KATHIRAVAN¹, INDRAJIT V. BARVE¹, G. K. BEEHARRY², AND G. N. RAJASEKARA²

¹ Indian Institute of Astrophysics, Bangalore 560 034, India; ramesh@iiap.res.in

² University of Mauritius, Reunion, Mauritius

Received 2010 March 17; accepted 2010 July 5; published 2010 July 20

ABSTRACT

We report observations of weak, circularly polarized, structureless type III bursts from the solar corona in the absence of H α /X-ray flares and other related activity, during the minimum between the sunspot cycles 23 and 24. The spectral information about the event obtained with the CALLISTO spectrograph at Mauritius revealed that the drift rate of the burst is ≈ -30 MHz s⁻¹ is in the range 50–120 MHz. Two-dimensional imaging observations of the burst at 77 MHz obtained with the Gauribidanur radioheliograph indicate that the emission region was located at a radial distance of $\approx 1.5 R_{\odot}$ in the solar atmosphere. The estimated peak brightness temperature of the burst at 77 MHz is $\sim 10^8$ K. We derived the average magnetic field at the aforementioned location of the burst using the one-dimensional (east–west) Gauribidanur radio polarimeter at 77 MHz, and the value is $\approx 2.5 \pm 0.2$ G. We also estimated the total energy of the non-thermal electrons responsible for the observed burst as $\approx 1.1 \times 10^{24}$ erg. This is low compared to the energy of the weakest hard X-ray microflares reported in the literature, which is about $\sim 10^{26}$ erg. The present result shows that non-thermal energy releases that correspond to the nanoflare category (energy $\sim 10^{24}$ erg) are taking place in the solar corona, and the nature of such small-scale energy releases has not yet been explored.

Key words: magnetic fields – Sun: activity – Sun: corona – Sun: radio radiation

1. INTRODUCTION

Solar flares occur over a wide range of energies: from $\sim 10^{29}$ erg for subflares to $\gtrsim 10^{32}$ erg for the largest flares. The frequency of flares continues to increase as we look at weaker and weaker energy releases. Lin et al. (1984), using high-sensitivity balloon-borne instrumentation, have detected weak hard X-ray spikes/bursts (called “microflares” since the energy involved was $\sim 10^{26}$ – 10^{28} erg) which are attributed to such energy releases. Microflares are of interest because of their possible bearing on the problems of coronal heating and solar flares. These events are impulsive and non-thermal. In addition to the aforementioned X-ray events, magnetic energy is released in several different forms that are not necessarily related to the traditional definition of flares (see Aschwanden 2004 for a recent review of the topic). In the radio domain, Kundu et al. (1986) reported small amplitude bursts at low frequencies (38.5, 50, and 73.8 MHz) related to weak energy releases in the solar corona. Similar observations were also reported at high frequencies (~ 1.4 GHz) by Bastian (1991). The characteristics of the low-frequency radio events in particular were similar to the commonly observed type III radio bursts from the solar corona, which are due to plasma emission (Wild 1950; Suzuki & Dulk 1985; White et al. 1987; Thejappa et al. 1990; Subramanian et al. 1993). It is now well understood that type III radio bursts result from streams of electrons traveling out from active regions along open magnetic field lines at a speed of about $c/3$. During their outward passage, the electron streams set up plasma oscillations (i.e., Langmuir plasma waves) at each height in the solar atmosphere. The frequency of oscillations is very nearly equal to the local plasma frequency f_p ($= 9 \times 10^{-3} n_{\text{th}}^{1/2}$, where f_p and the thermal electron density n_{th} are in units of MHz and cm⁻³, respectively). Some of the energy in the plasma waves is converted into propagating electromagnetic waves at both the fundamental and harmonic of the plasma frequency. The bursts observed by Kundu et al. (1986) were termed as “microbursts” since their peak brightness temperature (T_b) was $\sim 10^6$ K (White

et al. 1987; Thejappa et al. 1990) unlike the regular type III bursts whose average $T_b \sim 10^{10}$ K around 80 MHz (Suzuki & Dulk 1985). Recent numerical simulations by Li et al. (2009) indicate that type III bursts with different T_b values can be explained by varying the coronal and heating conditions in the region where they occur. For weak heating events or events with high coronal electron temperature, the simulations give rise to bursts with characteristics that quantitatively agree with microbursts. In this scenario, we present here the positional, spectral, and polarization information on a class of weak type III bursts with peak T_b intermediate to that of the microbursts and regular type III bursts mentioned above. The bursts were not accompanied by any activity in either H α or X-rays or microwaves.³ The estimated total energy in the non-thermal electrons that caused the burst in the present case was found to be about two orders of magnitude lower than the corresponding energy in the weakest ($\sim 10^{26}$ erg) hard X-ray microflares mentioned above.

2. OBSERVATIONS

The radio data reported were obtained with the heliograph (Ramesh et al. 1998) and the east–west one-dimensional polarimeter (Ramesh et al. 2008) at the Gauribidanur observatory,⁴ about 100 km north of Bangalore in India, and the CALLISTO spectrograph (Benz et al. 2005) at Mauritius. The heliograph (Gauribidanur radioheliograph, GRH) produces two-dimensional images of the solar corona while the polarimeter responds to the integrated and polarized flux densities of the whole Sun. Both the instruments can be used to simultaneously observe at different interference free spot frequencies in the range 40–120 MHz. But due to maintenance work, they were operated only at 77 MHz during the observing period reported here. The angular resolution of the GRH at the above frequency is $\approx 10' \times 15'$ (R.A. \times decl.). The CALLISTO spectrograph

³ <http://sgd.ngdc.noaa.gov/sgd/jsp/solarindex.jsp>

⁴ <http://www.iiap.res.in/centers/radio>

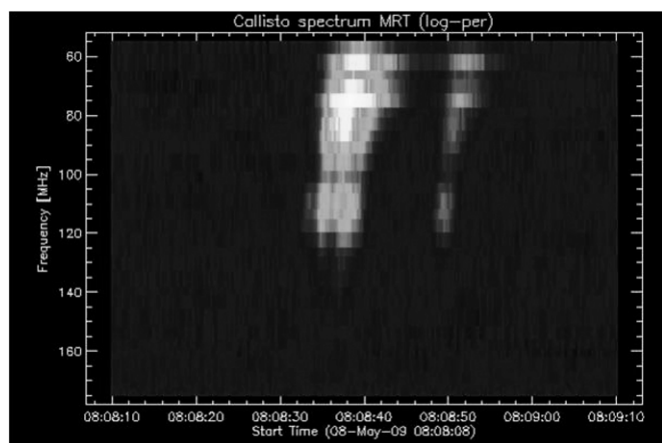


Figure 1. Dynamic spectrum of the two type III radio bursts observed with the CALLISTO radio spectrograph at Mauritius on 2009 May 8 during the interval 08:08:35–08:08:55 UT. The sweep time is ≈ 200 ms.

produces the dynamic spectrum of the radio emission from the whole Sun in the frequency range 45–870 MHz. The soft X-ray data were obtained with the X-ray sensor onboard the *Geostationary Operational Environmental Satellite (GOES 10)*.

Figure 1 shows the observations with the aforementioned radio spectrograph in the frequency range ≈ 50 –180 MHz during the period 08:08:10–08:09:10 UT on 2009 May 8. The two bright fast drifting features noticeable around 08:08:40 UT and 08:08:50 UT in the range ≈ 50 –120 MHz are the events under study. The drift rate is ≈ -30 MHz s^{-1} , which is nearly the same as the regular type III bursts (≈ -35 MHz s^{-1}) from the solar atmosphere in the above frequency range (Alvarez & Haddock 1973). Figure 2 shows the time profile of the soft X-ray (0.5–4 Å) flare energy from the whole Sun around the same time as the radio bursts in Figure 1. A comparison of Figures 1 and 2 indicates that the soft X-ray emission around the radio burst period was nearly close to the background value $\approx 1.1 \times 10^{-8}$ W m^{-2} . Obviously, no X-ray flares were reported.

Information on the location of the radio bursts in Figure 1 was derived from the GRH snapshot images (Figure 3) obtained at two different times during the burst interval, i.e., around

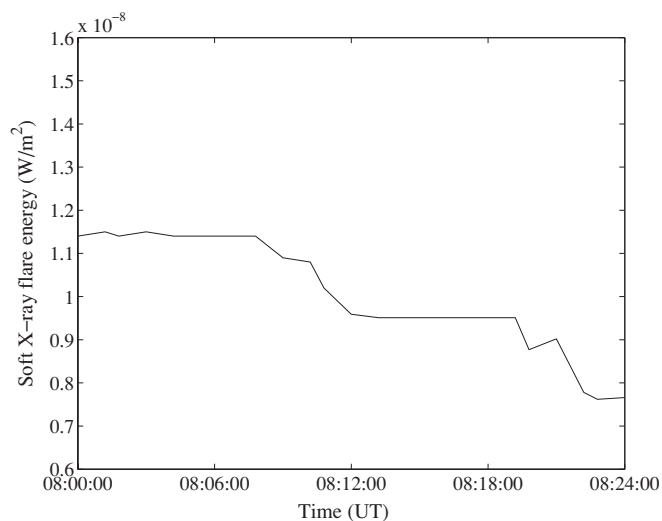


Figure 2. Soft X-ray (0.5–4 Å) flare energy observed from the whole Sun during the interval 08:00–08:24 UT on 2009 May 8 with the X-ray sensor onboard *GOES 10*. The integration time is ≈ 1 minute.

08:08:40 and 08:08:50 UT on 2009 May 8. One can note the burst as an intense, discrete source beyond the east limb of the Sun during both the above periods. Their peak T_b is $\approx 1.7 \times 10^8$ and 0.9×10^8 K at 08:08:40 and 08:08:50 UT, respectively. We measured the radial distance (r) of the centroid of the bursts in Figure 3 and found that $r \approx 1.5 \pm 0.2 R_\odot$ during both the aforementioned epochs. Since the bursts were located beyond the limb, these are likely to be close to the actual source heights (Gopalswamy et al. 1987). A shift in the source position due to ionospheric refraction effects is expected to be $\lesssim 0.1 R_\odot$ in the hour angle range ± 2 hr at 80 MHz (Stewart & McLean 1982). The hour angle corresponding to the observation presented here is ≈ 1 hr. Therefore, an error in the location of the bursts in Figure 3 due to the above problem is considered to be less. Similarly, effects of scattering (“irregular refraction”) on the observed source position/height are also considered to be small at 77 MHz compared to lower frequencies (Aubier et al. 1971). Ray tracing calculations employing more realistic coronal

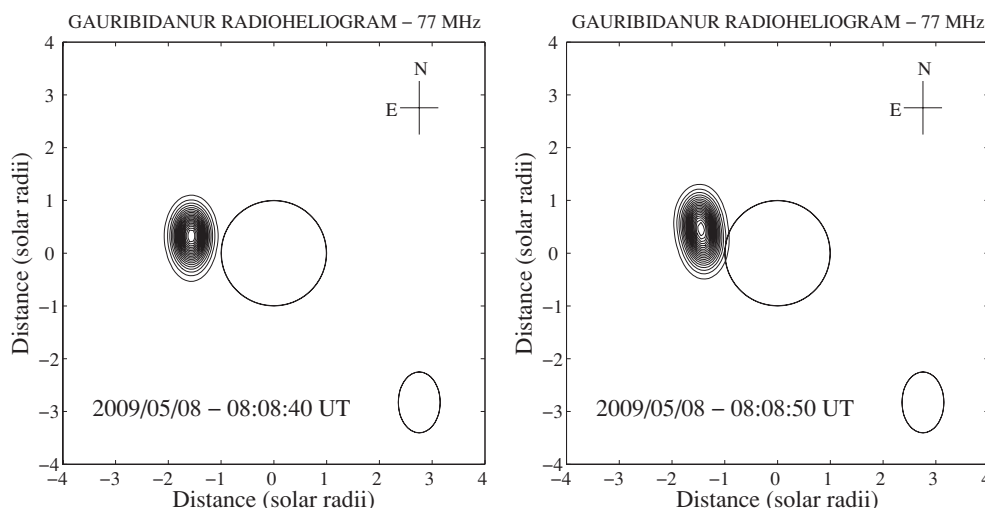


Figure 3. Snapshot images of the solar corona at 77 MHz obtained with the GRH on 2009 May 8 at 08:08:40 UT (left panel) and 08:08:50 UT (right panel). The integration time is ≈ 1 s. The estimated peak brightness temperatures (T_b) of the bursts are $\approx 1.7 \times 10^8$ and 0.9×10^8 K, respectively. The circle at the center in both the images represents the limb of the solar photosphere. The ellipse near the bottom right corner corresponds to the GRH beam size at 77 MHz.

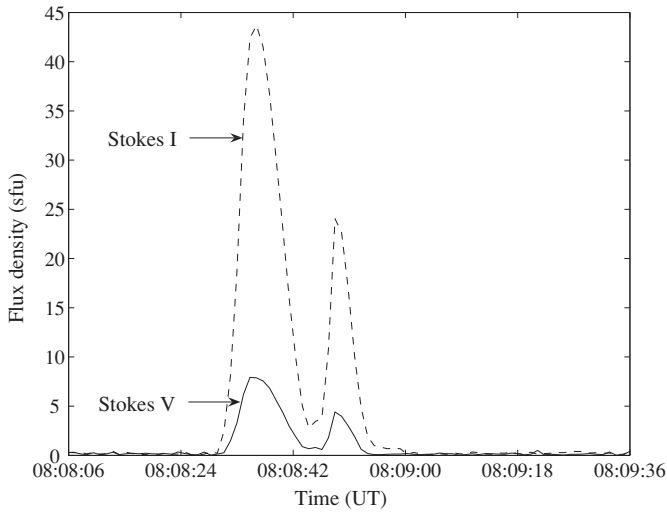


Figure 4. Time profile of the Stokes *I* & *V* emission observed from the Sun around the same time as the radio bursts in Figures 1 and 3, on 2009 May 8 at 77 MHz. The integration time is ≈ 1 s. The estimated dcp of the transient Stokes *V* emission, present immediately prior to as well as after 08:08:42 UT, is ≈ 0.18 .

electron density models and density fluctuations show that the turning points of the rays that undergo irregular refraction due to density inhomogeneities in the solar corona almost coincide with the location of the plasma (“critical”) layer in the non-scattering case even at 73.8 MHz (Thejappa & MacDowall 2008).

Figure 4 shows the responses of the polarimeter to the integrated (Stokes *I*) and the circularly polarized (Stokes *V*) flux densities on 2009 May 8 during the burst period in Figures 1 and 3. One can note that the burst is structureless in both Stokes *I* and *V*. The estimated peak degree of circular polarization ($dcp = V/I$) corresponding to the two events, present before and after the marker at 08:08:42 UT in Figure 4, is ≈ 0.18 . We presume that the bursts observed in the present case (Figure 1) are most likely due to second harmonic plasma emission because of the following reasons. (1) The source region is located beyond the limb of the Sun (Figure 3). Wild et al. (1959) pointed out that both the fundamental (F) and the harmonic (H) emission should generally be observable only for events near the center of the solar disk. Elsewhere it should be purely the H emission. This is because the F emission is more directive compared to the H emission. According to Suzuki & Sheridan (1982), the F component has a limiting directivity of $\pm 65^\circ$ (from the central meridian on the Sun) at 80 MHz. (2) The estimated values of dcp in the present case are close to the average dcp (≈ 0.11) reported for the circularly polarized H component of type III bursts. For the F component, the average dcp ≈ 0.35 (Dulk & Suzuki 1980). (3) The estimated peak T_b is $\sim 10^8$ K. According to Gopalswamy (1993), type III bursts with low polarization and no F–H structure (structureless bursts) are predominantly the H emission since the T_b of the F emission hardly exceeds a few times 10^5 K. (4) The observed drift rate of the bursts, their peak flux density, T_b , and life time are all consistent with that predicted for remote observations of the H emission of type III radio bursts at the Earth by the simulations of Li et al. (2009) using standard coronal electron density models. The authors also point out that the flux density levels of the F emission are too weak to be observed by typical radio instruments. A comparison with their results indicates that our observed values

of flux density and T_b at 77 MHz correspond to a coronal electron temperature (T_e) $\approx (2-3) \times 10^6$ K and an electron heating temperature (T_h) $\approx (20-25) \times 10^6$ K, at the source region.

3. RESULTS

We estimated the magnetic field at the source region of the bursts at 77 MHz using the polarimeter observations in Figure 4. Note that the presence of the background magnetic field at the source region of type III radio bursts can give rise to a net dcp in the ordinary (“o”) mode for the escaping radiation (see Melrose & Sy 1972; Melrose et al. 1978, 1980; Zlotnik 1981 for details). Presently, the polarization observations of the H component of type III radio bursts are considered to be a better diagnostic tool to estimate the solar coronal magnetic field since the polarization of the F component is affected by propagation effects (Dulk & McLean 1978). The polarization of the H component is related to the field strength via a simpler relationship (Suzuki & Sheridan 1978; Dulk & Suzuki 1980; Mercier 1990; Reiner et al. 2007). Melrose et al. (1978) and Zlotnik (1981) have derived the following empirical relationship between the coronal magnetic field B and the dcp of the H emission in the case of type III radio bursts, i.e.,

$$B = \frac{0.18f}{a(\theta)} \times dcp, \quad (1)$$

where f is the observing frequency and $a(\theta)$ is a slowly varying function of the angle θ between the magnetic field and the viewing direction. Its value is ~ 1 for emission regions near the solar limb (Dulk & McLean 1978). We assumed $a(\theta) \approx 1$ for the present calculations since the radio burst location at both 08:08:40 and 08:08:50 UT was close to the limb of the Sun (Figure 3). Substituting for f ($=77$ MHz) and dcp (≈ 0.18 corresponding to the first and second peaks in Figure 4) in Equation (1), we obtain $B \approx 2.5 \pm 0.2$ G, respectively.

Since the bursts reported were not accompanied by any activity in the other regions of the electromagnetic spectrum, we were interested in finding the total energy (E_{total}) of the non-thermal electrons responsible for the burst. For this we used the formula

$$E_{\text{total}} = n_{\text{th}}(n/n_{\text{th}})VE. \quad (2)$$

Here n_{th} is the number density of the background thermal electrons, n is the number density of the non-thermal electrons, V is the volume of the burst source, and E is the mean energy of the individual electrons. It has already been mentioned that the drift rate of the type III burst observed in the present case is ~ -30 MHz s^{-1} (Figure 1). Assuming Newkirk’s density model (Newkirk 1961) for the solar corona with a density enhancement factor of 2 (meant for the active region corona), we estimated the mean speed of type III electrons from the above drift rate and the value is $\approx 1.14 \times 10^8$ m s^{-1} . This corresponds to a mean energy (E) of ≈ 37 keV for the individual electrons. This is consistent with the values reported earlier for the electron energy associated with a harmonic type III burst in the similar frequency range (Gopalswamy & Kundu 1987). For the observing frequency of 77 MHz in Figure 3, $n_{\text{th}} \approx 7.32 \times 10^7$ cm^{-3} . Presuming the typical diameter of a magnetic loop to be $\approx 3'$ and the associated field strength as ≈ 1000 G close to the solar surface (Priest 1982), we estimated the width (w) of the loop at the height of the burst in the present case using the principle of magnetic flux conservation, i.e., $w = \sqrt{(1000/2.5) \times 9} \approx 4.4 \times 10^9$ cm. Taking the coronal scale height to be $\approx 10^{10}$ cm, we calculated the volume filled by the

non-thermal electrons responsible for the observed burst in the present case, and the value is $\approx 1.5 \times 10^{29} \text{ cm}^3$. For the number density (n) of non-thermal electrons, we used the simulations reported by Li et al. (2009) where the authors have calculated the variation of observed burst characteristics such as the peak T_b , the flux density (S), etc. with the fraction of electrons heated from T_e to T_h ($>T_e$) which leads to the formation of the electron beam that causes the burst. In the present case, $T_b \sim 10^8 \text{ K}$, and $S \approx 40 \text{ sfu}$ (1 sfu = solar flux unit = $10^{-22} \text{ W m}^{-2} \text{ Hz}^{-1}$). The value of n thus found is $\approx 5 \times 10^{-6}$. Substituting all these values in Equation (2), we obtain $E_{\text{total}} \approx 3.3 \times 10^{24} \text{ erg}$. As has been mentioned earlier, this is about 2 orders of magnitude lower than the energy of the weakest hard X-ray microflares reported in the literature. The present event probably belongs to the category of nanoflares pointed out by Parker (1988). The value of n_{th} mentioned above is also close to the typical density values of the nanoflare events (see, e.g., Aschwanden 2004).

4. CONCLUSION

We have reported observations of weak, circularly polarized, structureless radio bursts from the solar corona that were not accompanied by $\text{H}\alpha$ /X-ray flares or any other form of solar activity. The estimated magnetic field at the source region of the bursts at 77 MHz is $\approx 2.5 \pm 0.2 \text{ G}$. We calculated the non-thermal electron energy associated with the bursts as $\approx 3.3 \times 10^{24} \text{ erg}$. This is lower than the energy of the weakest hard X-ray microflares reported in the literature by about 2 orders of magnitude. The absence of any accompanying events at other regions of the spectrum in the present case could be due to the electron acceleration region being located comparatively high in the corona where $n_{\text{th}} \lesssim 10^8 \text{ cm}^{-3}$ (inferred from the starting frequency of $\approx 150 \text{ MHz}$ of the burst in Figure 1). This implies that the fraction of the accelerated electrons penetrating to the lower levels in the solar atmosphere from where the $\text{H}\alpha$ /hard X-ray activity generally occurs might be too small to produce detectable emission (see, e.g., Kane 1981). Note that the total energy of the non-thermal electrons at the aforementioned acceleration region is itself less ($\sim 10^{24} \text{ erg}$). Given this situation it looks like that regular observations of low-frequency radio events of the type reported might be a potential method for studying weak energy releases in the corona and for understanding the total energy budget of the corona and the solar wind in an independent manner (see, e.g., Parker 1988; Benz & Krüger 1995). Additionally, the present observations also signify the usefulness of radio observations to estimate the coronal magnetic field associated with such energy releases with good accuracy in a relatively straightforward manner.

We are grateful to A. O. Benz for kindly donating a CALLISTO radio spectrograph to the University of Mauritius and to C. Monstein for installing the same in Mauritius. We acknowledge National Geophysical Data Center (NGDC) for providing open access to GOES and other data through their Space Physics Interactive Data Resource (SPIDR) Web site. We profusely thank the referee for his/her comments which helped us to present our results more clearly.

REFERENCES

- Alvarez, H., & Haddock, F. T. 1973, *Sol. Phys.*, **29**, 197
 Aschwanden, M. 2004, *Physics of the Solar Corona—An Introduction* (Berlin: Springer)
 Aubier, M., Leblanc, Y., & Boischoit, A. 1971, *A&A*, **12**, 435
 Bastian, T. S. 1991, *ApJ*, **370**, L49
 Benz, A. O., & Krüger, A. 1995, *Coronal Magnetic Energy Releases*, Lecture Notes in Physics, Vol. 444 (Berlin: Springer)
 Benz, A. O., Monstein, C., & Meyer, H. 2005, *Sol. Phys.*, **226**, 121
 Dulk, G. A., & McLean, D. J. 1978, *Sol. Phys.*, **57**, 279
 Dulk, G. A., & Suzuki, S. 1980, *A&A*, **88**, 203
 Gopalswamy, N. 1993, *ApJ*, **402**, 326
 Gopalswamy, N., & Kundu, M. R. 1987, *Sol. Phys.*, **111**, 347
 Gopalswamy, N., Kundu, M. R., & Szabo, A. 1987, *Sol. Phys.*, **108**, 333
 Kane, S. R. 1981, *ApJ*, **247**, 1113
 Kundu, M. R., Gergely, T. E., Szabo, A., Loiacono, R., & White, S. M. 1986, *ApJ*, **308**, 436
 Li, B., Cairns, I. H., & Robinson, P. A. 2009, *J. Geophys. Res.*, **114**, A02104
 Lin, R. P., Schwartz, R. A., Kane, S. R., Pelling, R. M., & Hurley, K. C. 1984, *ApJ*, **283**, 421
 Melrose, D. B., Dulk, G. A., & Gary, D. E. 1980, *Proc. Astron. Soc. Aust.*, **4**, 50
 Melrose, D. B., Dulk, G. A., & Smerd, S. F. 1978, *A&A*, **66**, 315
 Melrose, D. B., & Sy, W. N. 1972, *Aust. J. Phys.*, **25**, 387
 Mercier, C. 1990, *Sol. Phys.*, **130**, 119
 Newkirk, G., Jr. 1961, *ApJ*, **133**, 983
 Parker, E. N. 1988, *ApJ*, **330**, 474
 Priest, E. R. 1982, *Solar Magneto-Hydrodynamics* (Dordrecht: Reidel)
 Ramesh, R., Kathiravan, C., SundaraRajan, M. S., Barve, I. V., & Sastry, Ch. V. 2008, *Sol. Phys.*, **253**, 319
 Ramesh, R., Subramanian, K. R., SundaraRajan, M. S., & Sastry, Ch. V. 1998, *Sol. Phys.*, **181**, 439
 Reiner, M. J., Fainberg, J., Kaiser, M. L., & Bougeret, J. -L. 2007, *Sol. Phys.*, **241**, 351
 Stewart, R. T., & McLean, D. J. 1982, *Proc. Astron. Soc. Aust.*, **4**, 386
 Subramanian, K. R., Gopalswamy, N., & Sastry, Ch. V. 1993, *Sol. Phys.*, **143**, 301
 Suzuki, S., & Dulk, G. A. 1985, in *Solar Radio Physics*, ed. D. J. McLean & N. R. Labrum (Cambridge: Cambridge Univ. Press), **289**
 Suzuki, S., & Sheridan, K. V. 1978, *Radiophys. Quantum Electron.*, **20**, 989
 Suzuki, S., & Sheridan, K. V. 1982, *Proc. Astron. Soc. Aust.*, **4**, 382
 Thejappa, G., Gopalswamy, N., & Kundu, M. R. 1990, *Sol. Phys.*, **127**, 165
 Thejappa, G., & MacDowall, R. J. 2008, *ApJ*, **676**, 1338
 White, S. M., Kundu, M. R., & Szabo, A. 1987, *Sol. Phys.*, **107**, 135
 Wild, J. P. 1950, *Aust. J. Sci. Res. A*, **3**, 399
 Wild, J. P., Sheridan, K. V., & Nylan, A. A. 1959, *Aust. J. Phys.*, **12**, 369
 Zlotnik, E. Ia. 1981, *A&A*, **101**, 250